Article:

Prélat, A, Pankhania, SS, Jackson, CA-L et al. (1 more author) (2015) Slope gradient and lithology as controls on the initiation of submarine slope gullies; Insights from the North Carnarvon Basin, Offshore NW Australia. Sedimentary Geology, 329. 12 - 17. ISSN 0037-0738

https://doi.org/10.1016/j.sedgeo.2015.08.009

Slope gradient and lithology as controls on the initiation of submarine slope gullies; insights from the North Carnarvon Basin, Offshore NW Australia

Prélat Amandine*, Pankhania Shyam S., Jackson Christopher A-L., and Hodgson David M.[1]**

Basins Research Group (BRG), Department of Earth Sciences and Engineering, Prince Consort Road, South Kensington Campus, Imperial College, London, UK

[1]Stratigraphy Group, School of Earth and Environment, University of Leeds, Leeds UK

* Now at Beicip-Franlab, 232 Avenue Napoléon Bonaparte, 92500 Rueil-Malmaison, France

****** Now at E.ON Exploration & Production, 129 Wilton Road, London, UK

ABSTRACT

Slope-confined submarine gullies are present on many continental margins, yet the controls on their initiation and demise are poorly understood because modern or recently active systems are rarely if ever monitored; and exhumed systems, typically formed in very fine-grained successions, are poorly preserved at outcrop. We use 3D seismic reflection and borehole data from offshore NW Australia to investigate long-term (~40 Myr) variations in the geomorphology of Eocene-to-Miocene gullies that developed in mixed carbonate-clastic clinothems. Through time, clinoform slope gradient increases from 1.6° to 3.2°, with gullies forming when the clinoform slope exceeds 2.5°. After their inception, gullies increase in width (from 350 m to 770 m) and depth (from 37 m to 60 m). Slope steepening appears to coincide with a change from poorly cemented, fine-grained

carbonate to better-cemented, coarse-grained carbonate, implying a secondary, lithological control on slope dip and, ultimately, gully formation.

KEYWORDS: shelf-edge clinoforms, slope gullies, mixed carbonate-clastic system

INTRODUCTION

Submarine slope-confined gullies (i.e. gullies restricted to the slope, between the shelf edge and the toe-of-slope) are common on many clastic- (e.g. Chiocci and Normark, 1992; Jobe et al., 2011, Surpless et al., 2009) and carbonate-dominated continental margins (e.g. Mulder et al., 2012). In cross-section, they are 'V'- or 'U'-shaped, and are typically narrower, shorter and of lower relief than submarine channels or canyons (Field et al., 1999; Jobe et al., 2011; Lonergan et al., 2013). Gullies are orientated broadly normal to the slope and form conduits for sediment transport from the shelf edge toward the deep basin. In contrast to submarine channels, gullies commonly occur in evenly-spaced groups, and their stacking patterns are dominantly aggradational (e.g. Lonergan et al. 2013). Submarine gullies are thought to initiate and evolve in response to erosion by shelf-derived turbidity currents (Lonergan et al., 2013; Micallef and Mountjoy, 2011; Weaver et al., 2000) and/or retrogressive slope failure (Gardner et al., 1999). Because most gullies form in, and are filled by, very fine-grained successions, it is often difficult to constrain their morphology and thus their stratigraphic evolution using outcrop data (Hubbard et al., 2010; Jones et al. 2015). Rare coarse-grained filled gullies have been studied recently but the mechanisms leading to their formation remain poorly constrained (e;g. Di Celma et al., 2013; Surpless et al., 2009). Furthermore, seabed-imaging techniques only permit analysis of the present form and not the long-term evolution of gullies (Field et al., 1999; Lonergan et al., 2013). Finally, because oceanographic currents and sediment gravity currents are difficult to monitor directly, their role in gully initiation and evolution is poorly constrained.

We here use high-quality 3D seismic reflection, well-log and cuttings data from the Northern Carnarvon Basin (NCB), offshore NW Australia to explore some of the potential mechanisms controlling the initiation and long-term (~40 Myr) evolution of submarine slope-confined gullies. This study area was selected because it is characterised by an areally extensive, high-quality 3D seismic reflection dataset that allows us to: (1) constrain the dip and strike architecture of Eocene-to-Miocene continental margin-scale (i.e. several hundred metres tall) gully-bearing clinothems (Fig. 1); and (2) constrain the morphology, stratigraphy and distribution of slope-confined gullies. Such an extensive view (areally and temporally) of the development of slope gullies and their host clinoforms is typically not afforded by outcrop dataset (Di Celma et al., 2013; Surpless et al. , 2009). Furthermore, the availability of well-logs and cuttings data, which are not often available in shallow subsurface datasets, allows us to constrain the lithology and age of the gully-bearing successions, and, for the first time, the remarkable longevity (>40 Myr) of slope gullies.

GEOLOGICAL SETTING

The NCB is located offshore NW Australia and developed in response to extension during late Permian to early Mesozoic (Bradshaw et al., 1998; Langhi and Borel, 2005). Post-Jurassic, post-rift thermal subsidence was interrupted by a minor phase of inversion during the Late Cretaceous (Veevers et al., 1991). We focus on shelf-margin clinothems that prograded north-westwards into the NCB during the Eocene and Miocene (Fig. 1 and 2). The clinothems are composed predominantly of transported temperate carbonate grains (e.g. calcisiltite, calcilutite and calcarenite), and unconsolidated fine-grained carbonate (e.g. marl), locally cemented by dolomite (Fig. 3) (Cathro et al., 2003; Moss et al., 2004). Siliciclastic material is restricted to the Late Miocene shelf interval (see well Goodwyn 6 in Fig. 3), supplied by deltas that reached the shelf edge during sea-level lowstands following the Middle Miocene Climatic Optimum (Molnar, 2004; Sanchez et al., 2012). Large Cenozoic fluvial systems have not been identified on this part of the margin, suggesting that these deltas and shelf sands were supplied by small rivers not imaged on seismic reflection data (Sanchez et al., 2012).

DATASET AND METHODOLOGY

This study utilises two time-migrated, 3D seismic reflection datasets that cover ~2500 km^2 (Rosie and Demeter; Fig. 1). Crossline and inline spacing are 12.5 m and 25 m respectively within Demeter, and 18.75 m within Rosie. Both datasets are zero-phase processed; a downward increase in acoustic impedance is represented by a peak (red) reflection. In the interval of interest, central frequencies are 32-50 Hz and acoustic velocities are ~3200 m.s^{-1}, resulting in a vertical resolution of 15-20 m and a horizontal resolution of 15 m. Vertical measurements (e.g. clinoform height, gully depth) are depth converted using an average velocity of 3200 m s^{-1} (Cathro et al., 2003).

We mapped 12 key seismic horizons (H1-H12; Fig. 2 and 4). H1 and H12 define the base and top, respectively, of the NW-dipping clinoform-bearing succession. Intervening horizons were chosen because of their lateral continuity and stratigraphic position within the studied succession. Morphometric analysis of the clinoform-bearing succession were conducted on four dip-orientated (NW-SE) seismic profiles (for methodology, refer to Cathro et al., 2003). Our morphometric analysis focused on clinoform height, length and declivity; individual clinoforms were defined updip by the break in slope at the clinoform rollover (crudely correlating to the shelf edge; i.e. yellow points on Fig. 2) and downdip by the break in slope defining the transition between the clinoform slope and bottomset (i.e. green points on Fig. 2). A variance attribute is used to highlight gully location and geometry on key horizons (Fig. 1). Gully width and depth, along with stacking and spacing (i.e. distance between thalwegs of neighbour gullies) are used to define changes in gully morphology. Height measurements are compacted values.

Well logs, cuttings and well completion reports from three wells are used to ascertain the lithology of the Eocene-Miocene interval (Goodwyn 6, Echo 1, and Eastbrook 1; Fig. 1). Detailed foraminifera analysis provides age duration of the studied succession and helps to constrain margin progradation rates and the period of gully development (see Cathro et al., 2003; Moss et al., 2004) (Fig. 3).

RESULTS

We identify three units (A-C) based on the amount and morphology of the gullies they contain. The bounding horizons define important changes in gully morphology, scale and stacking pattern. Unit A consists of smooth clinoforms that lack gullies, unit B contains relatively narrow and shallow, aggradational and slope-confined gullies, and unit C contains relatively wide and deep slope-confined gullies that aggrade and migrate laterally through time. Clinoform and gully geometry in units A-C are described below.

Unit A

Unit A (Eocene-to-Lower Miocene) contains clinoforms (n=17) that are on average 230 m high, 4.8 km long and dip 1.6°-2.5° (average 2.2°; Fig 2). Approximately 13 km of margin progradation and 350 m of aggradation occurred during deposition of unit A (Fig. 2), giving an average progradation rate of 540 m My^{-1} and aggradation rate of 17 m My^{-1} for this part of the margin. Clinoforms are relatively smooth (Fig. 4A), lack gullies and get taller and steeper through time (Fig. 2).

Penetration of the slope (Goodwyn 6), the slope-to-bottomsets transition (Echo 1) and bottomsets (Eastbrook 1) of unit A (Fig. 2) indicates that H1 generally represents an important change in lithology from clastics (claystone) to carbonates (Fig. 3). Sidewall cores and cuttings indicate that, across the entire shelf-to-basin floor profile, unit A is dominated by fine-grained transported carbonate deposits and marl, with subordinate calcarenite (Moss et al., 2004) (Fig. 3). In Goodwyn 6, only small amounts (up to 20%) of skeletal material are present in a poorly cemented calcilutite (Moss et al., 2004).

Unit B

Unit B (Middle Miocene) contains clinoforms (n=12) that are on average 445 m tall, 6.2 km long, and have steeper foresets (2.0°-3.2°, average of 2.5°) than those in unit A (Figs. 2). Approximately 2.6 km of margin progradation and 240 m of aggradation occurred during deposition of unit B (Fig. 2), yielding an average progradation and aggradation rate of 590 m My^{-1} and 54 m My^{-1} respectively. Foresets in unit B contain numerous gullies (n=30), which are 285-420 m wide (average 350 m) and 31-43 m deep (average 37 m). Gullies are relatively straight and spaced 520-910 m (average 715 m, n=20). Gullies in unit B are commonly vertically stacked and little to no erosion is observed at their base, with a net aggradation of 240 m recorded (Fig. 4B).

The topsets (Goodwyn 6), foresets (Echo 1) and bottomsets (Eastbrook 1) of unit B clinoforms are penetrated by wells (Fig. 2), indicating that the shelf and slope of unit B is dominated by calcarenite, whereas calcilutite and calcisiltite dominate on the basin floor (Fig. 3, Moss et al., 2004). Sidewall cores and cuttings indicate that calcarenites on the shelf and slope are richer (30%) in skeletal fragments, and calcite and/or carbonate cement (15%) than in unit A, corresponding to an influx of larger foraminifera, corals and bivalves in the Middle Miocene (Hocking et al., 1987; Moss et al., 2004). Data from Goodwyn 6 indicate that the Middle Miocene (Unit B) was the time of maximum sediment accumulation rate (see interval EMM1 and MM of Moss et al. 2004).

Unit C

Unit C (Upper Miocene) contains clinoforms that have strongly gullied foresets (Fig. 2 and 4). Clinoforms (n=10) are on average 600 m high, 12.8 km long, and dip more gently than in units A and B (1.5°-1.6°, average of 1.5°) (Fig. 2). The margin prograded ~5.3 km and aggraded ~170 m during deposition of unit C, yielding an average progradation and aggradation rate of 1380 m My^{-1} and of 44 m My^{-1} respectively, the former being >2 times higher than during deposition of unit B and the latter being broadly equal. Gullies are 535-1020 m wide (average 775 m, n=21), 51-68 m deep (average 60 m, n=21) and spaced 1035-2670 m (average 1850 m, n=21). Although unit C gullies are net-aggradational, many have erosive bases along their entire dip extent, which is illustrated in cross section by strongly erosive reflectors, cutting out older stratigraphy (Fig. 4C). Unit C gullies are wider and deeper than those in unit B and are laterally offsetstacked, which contrasts with the weakly erosional and aggradational gullies developed in unit B (Fig. 4B-C).

The topsets (Goodwyn 6 and Echo 1), and topsets-to-foresets (Eastbrook 1) of unit C clinoforms are penetrated by wells (Fig. 2). In Goodwyn 6, unit C is characterised by calcarenite with a thick (70 m) dolomite capped by two thick (70-90 m) fine- to medium grained sandstones (Fig. 3). In Echo 1, the dominant facies is similar to that found in unit B (calcarenite). In Eastbrook 1, the dominant facies is similar to that found in unit A and B (calcilutite and calcisiltite), but is richer in skeletal fragments (20-50%) and carbonate cement (5-20%) (Moss et al., 2004).

DISCUSSION

Several mechanisms may have been involved in the initiation of slope-confined gullies on continental margins. For example, erosion at the base of sediment-poor cascading dense waters, mass-wasting via retrogressive failure and erosional scour at the base of turbidity currents can form gullies (Spinelli and Field, 2001; Izumi, 2004; Micallef and Mountjoy, 2011; Mulder et al., 2012). These processes can be driven by an increase in sediment supply caused by increasing proximity to a shelf delta, by sea level variations caused by climatic changes or tectonically induced uplift and subsidence, and by changes in the oceanographic regime. Because no data are available on oceanic current circulation or tide-generated currents during the Eocene-Miocene of NW Australia, and these processes are almost impossible to infer from 3D seismic reflection and well data alone, we are not able to evaluate their potential role in the development of the gullies identified here. We instead discuss two linked factors that we believe have contributed to the initiation of slope-confined gullies in the NCB: changing slope dip and lithology.

Seismic data indicate that clinoform dip increases from 1.5° in unit A to >2.5° in unit B. The change in dip is accompanied by a change in clinoform stacking pattern, from dominantly progradational to dominantly aggradational (Fig. 2). Unit B (54 m My^{-1}) is also characterised by a higher aggradation rate than unit A (17 m My^{-1}) whereas the progradation rate is similar (590 m My^{-1} in B; 540 m My^{-1} in A). However, both aggradation and progradation rates for units A and B remain low compared to clastic margins (up to 2500 m My^{-1} of aggradation and 60 km My^{-1} of progradation; Carvajal et al. 2009). Gully initiation occurred in unit B when clinoform dip reached and then exceeded 2.5°. Here, we speculate that this dip increase contributed to gully initiation in one of two ways. First, above 2.5°, the slope was in disequilibrium and thus unstable, triggering a sequence of retrogressive failures (Izumi, 2004). However, no failure scars, which may have represented the precursor to gully formation, are observed below or within unit B. Second, an increase in dip may have resulted in a reduction of the 'contributing length' (Micallef and Mountjoy, 2011), which is the distance required for flows to ignite and be capable of entraining seafloor sediment. A reduction in the contributing length by slope steepening enabled flows to entrain sediment and create gullies. Although minor slope erosion is likely an important contributor to the formation of gullies, net deposition outside and on the flanks of these erosional fairways results in net slope aggradation (see also Jobe et al., 2012; Lonergan et al., 2013).

An increase in slope dip from unit A to B is accompanied by an increase in grain-size (from calcilutite and calcisiltite to calcarenite), an increase in cementation (from poorly cemented up to 20% of carbonate cement), and an increase in the proportion of skeletal fragments (from 0 to 50%). We suggest that this change in lithology, and cementation state, helped the construction of higher, steeper slopes (from ~230 m in A to ~445 m in B, and from 2.2° in A to 2.5° in B) (Fig. 2A and 3) (cf. Kenter, 1990; Schlager and Camber, 1986).

Unit C is characterised by wider, deeper and more erosive gullies than unit B, which developed on foresets that dip <2.5°. Therefore, once they formed, gully maintenance and growth appears to be independent of slope steepness. We speculate that other factors controlled not only the persistence, but also the growth of gullies. For example, increased clastic sediment supply to the outer shelf and slope in the Late Miocene, related to the Middle Miocene Climatic Optimum, may have caused gully deepening and widening, as turbidity currents became focused in only few of the gully related bathymetric lows (Lonergan et al., 2013; Moss et al., 2004) (see well Goodwyn 6 in Fig. 3). These flows may have been as frequent and erosive as those that formed gullies in unit B, but, by virtue of being more focused due to flow entrapment in the progressively enlarging erosional conduits, gullies in unit C were wider and deeper than those in unit B. Alternatively, the flows during unit C times may have been less frequent, but larger, more turbulent and more erosive. Hocking et al. (1987) noted the increased occurrence of coarse sandstone within basinal facies (such as in Eastbrook 1) throughout the Upper Miocene (i.e. unit C) succession; we suggest that these sandstones are the basinal equivalent of the thick deltaic sandstones penetrated on the shelf (Goodwyn 6; Fig. 3).

CONCLUSIONS

We use 3D seismic and well data to document the initiation, geometry and evolution of Eocene-Miocene, slope-confined gullies in the NCB, and their genetic link to shelf margin clinoforms on which they are developed. Sediments accumulated offshore NW Australia are carbonate-dominated, which explain the overall low aggradation and progradation rates of the margin during the Eocene-to-Miocene, compared to clastic margins. Gullies initiated as narrow (~350 m wide), shallow (~37 m deep), closely spaced (~715 m) aggradational conduits (unit B), before becoming wider (~775 m), deeper (~60 m), more widely spaced (~1850 m) erosional conduits (unit C). We speculate that gully formation is linked to an increase in slope gradient caused by an increase in grain size and cementation. We have argued that, in this case, slope gullies appear to have needed a foreset gradient threshold of >2.5° to initiate. The sedimentary processes involved in the transfer of sediments from the slope to the basin floor are unknown. Gullies are not limited to steep slopes, and, during the Upper Miocene, they form on slopes of <2.5°. We thus postulate that other factors, possibly including increase sediment flux to the slope, are needed to widen and deepen slope confined submarine gullies.

ACKNOWLEDGMENTS

The authors wish to acknowledge Geoscience Australia for providing the data used here. Carl Jacquemyn is thanked for helpful discussions and comments on an earlier version of the manuscript. Asu Fubara is thanked for initial work on the Rosie seismic dataset. Journal reviewer Steve Hubbard and associate editor Brian Jones are gratefully acknowledged for their thoughtful contribution and helpful criticism that sharpened the manuscript.

REFERENCES

Bradshaw, M.T., Yeates, A.N., Beynon, R.M., Brakel, A.T., Langford, R.P., Totterdell, J.M. and Yeing, M. (1998) Paleogeographic evolution of the North West Shelf region. In: The North West Shelf, Australia (Eds P.G

Purcell and R.R Purcell), Proceedings of Petroleum Exploration Society Australia Symposium, Perth, 29-54.

Carvajal, C., Steel, R., and Petter, A. (2009). Sediment supply: the main driver of shelf-margin growth. Earth Science Reviews, 96 (4), 221-248.

Cathro, D.L., Austin, J.A. and Moss, G.D. (2003) Progradation along a deeply submerged Oligocene-Miocene heterozoan carbonate shelf: How sensitive are clinoforms to sea level variations? AAPG Bulletin, 87, 1547-1574.

Chiocci, F.L. and Normark, W.R. (1992) Effect of sea-level variation on upper-slope depositional processes offshore of Tiber delta, Tyrrhenian Sea, Italy. Marine Geology, 104, 109-122.

Di Celma, C., Cantalamessa, G. and Didaskalou, P. (2013) Stratigraphic organization and predictability of mixed coarse-grained and fine-grained successions in an upper slope Pleistocene turbidite system of the Peri-Adriatic Basin. Sedimentology, 60, 763–799.

Field, M.E., Gardner, J.V. and Prior, D.B. (1999) Geometry and significance of stacked gullies on the northern California slope. Marine Geology, 154, 271-286.

Gardner, J.V., Prior, D.B. and Field, M.E. (1999) Humboldt slide - a large shear-dominated retrogressive slope failure. Marine Geology, 154, 323-338.

Hocking, R.M., Moors, H.T. and Van De Graaff, W.J.E. (1987) Geology of the Carnarvon Basin Western Australia. Geological Survey of Western Australia, Bulletin 133.

Hubbard, S.M., Fildani, A., Romans, B.W., Covault, J.A. and McHargue, T. (2010) High-relief slope clinoform development: insight from outcrop, Magallanes Basin, Chile. Journal of Sedimentary Research, 80, 357-375.

Izumi, N. (2004) The formation of submarine gullies by turbidity currents. Journal of Geophysical Research, 109, C03048.

Jobe, Z.R., Lowe, D.R. and Uchytil, S.J. (2011) Two fundamentally different types of submarine canyons along the continental margin of Equatorial Guinea. Marine and Petroleum Geology, 28, 843-860.

Jones, G.D., Hodgson, D.M., and Flint, S.S. (2015) Lateral variability in clinoform trajectory, process regime, and sediment dispersal patterns beyond the shelf-edge rollover in exhumed basin margin-scale clinothems. Basin Research. DOI: 10.1111/bre.12092

Kenter, J.A.M. (1990) Carbonate plateforms flanks: slope angle and sediment fabric. Sedimentology, 37, 777-794.

Langhi, L. and Borel, G.D. (2005) Influence of the Neotethys rifting on the development of the Dampier Sub-basin (North West Shelf of Australia), highlighted by subsidence modelling. Tectonophysics, 397, 93-111.

Lonergan, L., Jamin, N.H., Jackson, C.A.-L., and Johnson, H.D. (2013) U-shaped slope gully systems and sediment waves on the passive margin of Gabon (West Africa). Marine Geology, 337, 80-97.

Micallef, A. and Mountjoy, J.J. (2011) A topographic signature of a hydrodynamic origin for submarine gullies. Geology, 39, 115-118.

Molnar, P. (2004) Late Cenozoic increase in accumulation rates of terrestrial sediment: How might climate change have affected erosion rates? Annual review of Earth and Planetary Sciences, 32, 67-89.

Moss, G.D., Cathro, D.L. and Austin Jr, J.A. (2004) Sequence biostratigraphy of prograding clinoforms, northern Carnarvon Basin, Western Australia: a proxy for variations in Oligocene to Pliocene global sea level? Palaios, 19, 206-226.

Mulder, T., Ducassou, E., Eberli, G.P., Hanquiez, V., Gonthier, E., Kindler, P., Principaud, M., Fournier, F., Léonide, P., Billeaud, I., Maresset, B., Rejmer, J.J.G., Bondu, C., Joussiaume, R. and Pakiades, M. (2012) New insights into the morphology and sedimentary processes along the western slope of Great Bahamas Bank. Geology, 40, 603-606.

Sanchez, C.M., Fulthorpe, C.S., and Steel, R.J. (2012) Middle Miocene-Pliocene siliciclastic influx across a carbonate shelf and influence of deltaic sedimentation on shelf construction, Northern Carnarvon Basin, Northwest shelf of Australia: Basin Research, 24, 1-19.

Schlager, W. and Camber, O. (1986) Submarine slope angles, drowning unconformities, and self-erosion of limestone escarpments. Geology, 14, 762-765.

Spinelli, G.A. and Field, M.E. (2001) Evolution of continental slope gullies on the northern California margin. Journal of Sedimentary Research, 71, 237-245.

Surpless, K.D., Ward, R.B., and Graham, S.A. (2009). Evolution and stratigraphic architecture of marine slope gully complexes: Monterey Formation (Miocene), Gaviota Beach, California. Marine and Petroleum Geology, 26 (2), 269-288.

Veevers, J.J., Powell, C.M. and Roots, S.R. (1991) Review of seafloor spreading around Australia, Synthesis of the patterns of spreading. Australian Journal of Earth Sciences, 38, 373-389.

Weaver, P.P.E., Wynn, R.B., Kenyon, N.H. and Evan, J.M. (2000) Continental margin sedimentation, with special reference to the north-east Atlantic margin. Sedimentology, 47, 239-256.

FIGURE CAPTIONS:

Figure 1. Variance extraction along H9 showing the plan-view expression of slope-confined gullies (high variance values are red to yellow). The location of the wells and the seismic profiles shown in figures 2 and 4A-C are indicated. G6 = Goodwyn 6, Ec1 = Echo 1 and E1 = Eastbrook 1. Inset map shows the location of the study area (red box) with respect to Australia.

Figure 2. A. Graph illustrating clinoform foreset dip, length and height. B. Dip-orientated (NW-SE) geoseismic section showing the cross-sectional expression of gully-free (i.e. unit A) and gully-prone (i.e. units B and C)

clinoforms and the seismic-stratigraphic framework employed in this study. Locations of wells Goodwyn 6, Echo 1 and Eastbrook 1 are shown.

Figure 3. Stratigraphic correlation between wells Goodwyn 6, Echo 1, and Eastbrook 1. The 12 key seismic horizons and three main seismic units (A-C) are shown. Available biostratigraphy is shown for each well (data from Moss et al., 2004).

Figure 4. Uninterpreted strike-orientated (NE-SW) seismic section through: A. unit A slope, B. unit B slope, and C. unit C slope. Note that unit A consists of continuous reflections, unit B is characterised by aggradational, shallow, narrow gullies, and unit C is characterised by erosional, deeper, wider gullies. Velocity pull-ups (vpu) are observed within unit B, presumably due to faster velocities in material filling overlying unit C gullies. Yellow arrows show dominant direction of gully stacking.

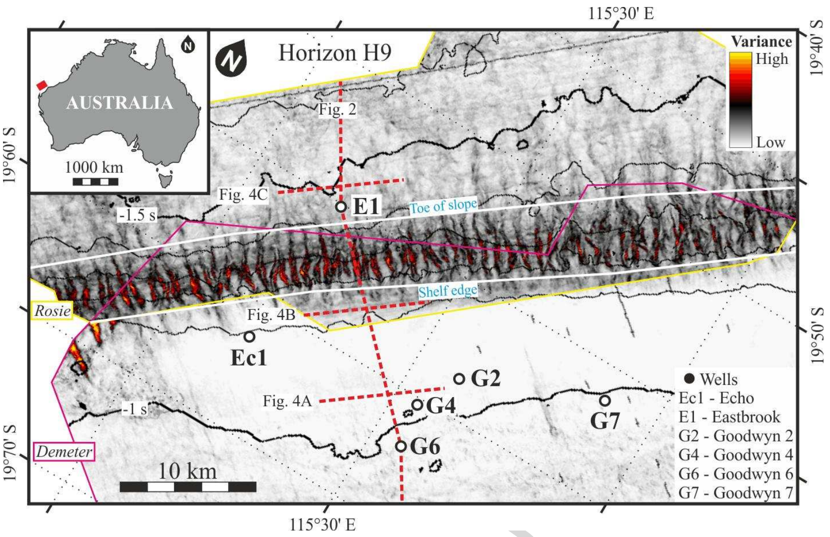

Fig. 1

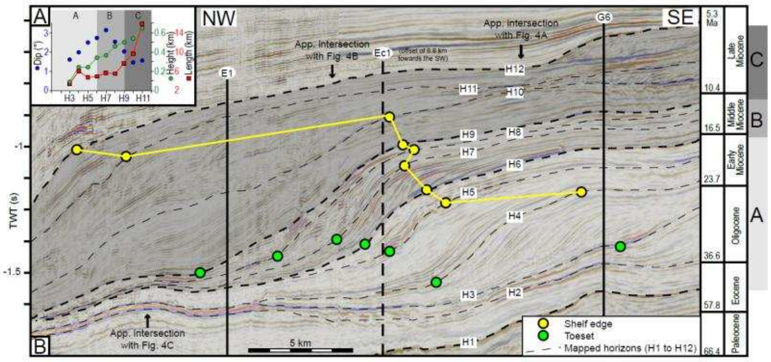

Fig. 2

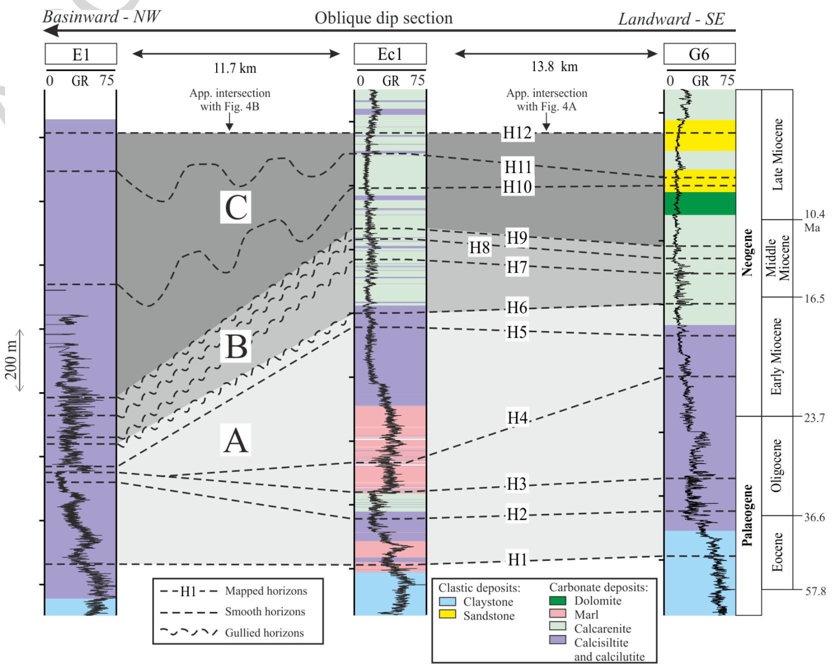

Fig. 3

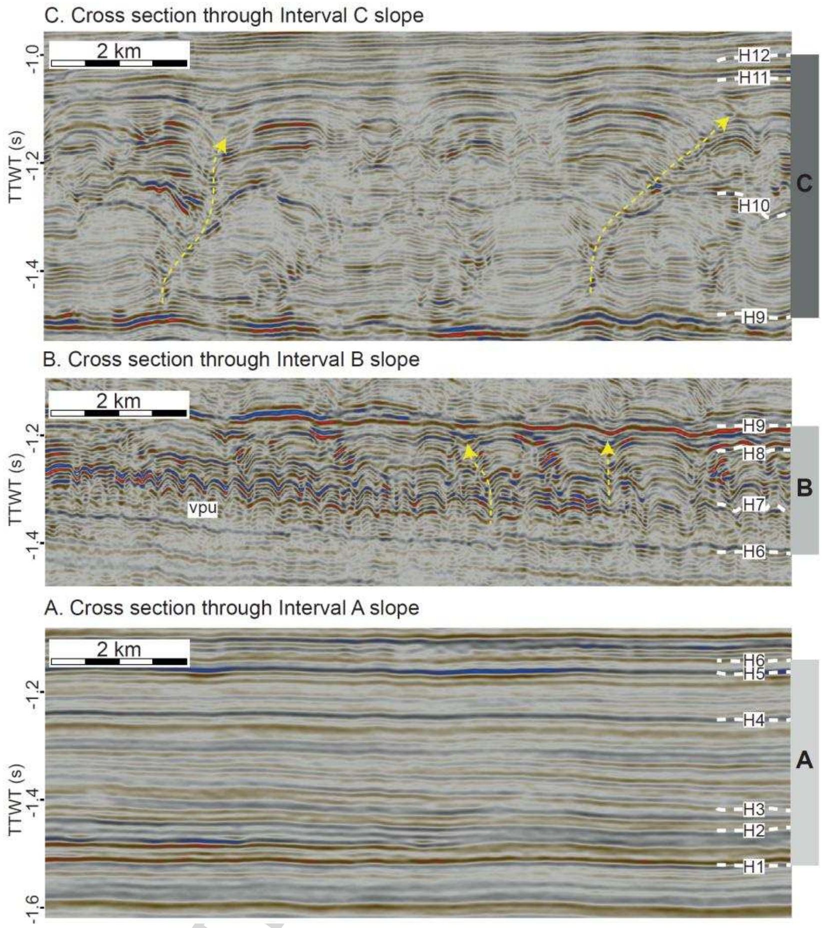

C. Cross section through Interval C slope
2 km
-1.0
-1.2
-1.4
TTWT (s)
H12
H11
H10
H9
C
B. Cross section through Interval B slope
2 km
-1.2
-1.4
TTWT (s)
vpu
H9
H8
H7
H6
B
A. Cross section through Interval A slope
2 km
-1.2
-1.4
-1.6
TTWT (s)
H6
H5
H4
H3
H2
H1
A

Fig. 4